

Kinetic parameters of Al–Si spinel crystallization from Algerian tamazarte kaolin

FOUDIL SAHNOUNE^{1,2*}, DJAIDA REDAOUI² AND MESSAOUD FATMI¹

¹Research Unit on Emerging Materials (RUEM), Ferhat Abbas of Setif 01,
Setif 19000, Algeria

²Physics Department, Faculty of Science, University of M'sila,
28000 M'sila, Algeria

Received: August 23, 2016; Accepted: November 22, 2016.

In this study, the mechanism and kinetic parameters of Al–Si spinel crystallization from Algerian Tamazarte kaolinite was studied by Differential thermal analysis (DTA) technique, which were carried out on samples between room temperature and 1400°C at different heating rates (10–40°C/min). X-ray diffraction was used to identify the phases present in the samples. The activation energies measured by both isothermal (Johnson–Mehl–Avrami (JMA) theory using Ligeró method) and non-isothermal (Kissinger methods) treatments are 870 and 810 kJ/mol, respectively. The growth morphology parameters n (Avrami parameter which indicates the crystallization mode) were found to be almost equal to 1.08, using non-isothermal treatments, and equal to 1.17 using isothermal (Ligeró method) and m (the numerical factor which depends on the dimensionality of crystal growth) was 1.07 obtained by Matusita and al. equation. Analysis of the results showed that bulk nucleation was dominant in Al–Si spinel crystallization followed by two-dimensional growth of mullite crystals with plates morphology controlled by diffusion from a constant number of nuclei.

Keywords: Kaolin, Differential thermal analysis, Avrami parameter, Activation energy, Kinetic parameters, Al–Si spinel.

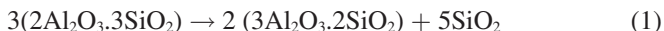
1 INTRODUCTION

Kaolin is usually utilized in a various number of applications such as sintered ceramic compositions, the ceramic industry which contained: structural and refractory ceramic, conventional ceramics, microwave dielectrics,

*Corresponding author: sahnounefoudil@yahoo.com

high-temperature protective coatings, infrared transmitting materials and microelectronic packaging. Further than the ceramics, Kaolin is used an industrial filler agent for paper rubber, cosmetics, paints, plastics, etc. Additionally, it can be utilized for waste management and preparation of geopolymers and geopolymer with based composites, zeolites and intercalates [1–3].

All these applications involve the importance of the thermal transformation of kaolin [1], the main mineral constituent of kaolin is kaolinite ($\text{Al}_2\text{Si}_2\text{O}_5(\text{OH})_4$ or $\text{Al}_2\text{O}_3 \cdot 2\text{SiO}_2 \cdot 2\text{H}_2\text{O}$ by oxide formula). In nature, kaolinite usually varies to a great extent in their crystalline order of perfection and particle. Hence kaolinite contains different types of impurities, e.g., quartz, mica, illite, feldspar, TiO_2 , and Fe_2O_3 as associated phases are habitually related with clays of different localities [4], the formation of Al–Si spinel phase $3\text{Al}_2\text{O}_3 \cdot 2\text{SiO}_2$ from metakaolin $\text{Al}_2\text{O}_3 \cdot 2\text{SiO}_2$ at 1050°C described by the equation (1) as follows [5,6]:



Many published works [3,6,7] support the formation Al–Si spinel that is one of intermediates of mullite rising during thermal treatment of kaolinite. In the present integrative study, the crystallization kinetics and growth mechanism of Al–Si spinel formation were studied using thermogravimetric analysis (TG), differential thermal analysis (DTA), differential scanning calorimetry (DSC) and X-ray diffractometer (XRD).

The aim of this paper is to study the crystallization kinetics of Al–Si spinel phase from Algerian Tamazarte kaolin have been investigated by DTA in order to estimate the activation energy of Al–Si spinel formation based on isothermal and non-isothermal methods, the growth morphology parameters n and m and the frequency factor for the reaction of Al–Si spinel.

2 MATERIALS AND METHODS

Starting materials used in this investigation were raw kaolin of Tamazarte (KT) (from Jijel, Algeria) with the chemical compositions was listed in Table 1. The KT kaolin also contains the impurities metal oxides. A high content (2.96%) of K_2O comes from the residual muscovite mica. The raw kaolin was milled by using planetary ball mill with alumina grinding media for 5 h the raw kaolin then milled for 2 h using ZrO_2 balls (diameter of 1.25 mm) by attrition way at a speed of $700 \text{ rev} \cdot \text{min}^{-1}$. The slurry was dried at 150°C , powdered after that sieved through a $63 \mu\text{m}$ mesh.

Thermal behaviors were measured by TG/DSC instruments (Setaram LABSYS Evo TG-DSC 1600°C equipment) at a heating rate of 10, 15, 20, 25, 30, 35 and $40^\circ\text{C}/\text{min}$ under flow of argon gas ($40 \text{ cm}^3 \cdot \text{min}^{-1}$). X-ray

TABLE 1
Chemical composition of the raw kaolin (wt. %)

Al ₂ O ₃	SiO ₂	Na ₂ O	P ₂ O ₅	SO ₃	K ₂ O	MgO	CaO	Fe ₂ O ₃
33.00	61.73	0.14	0.03	0.03	2.96	0.44	0.44	0.80

diffraction analysis was carried out on diffractometer system (XPERT-Pro) using Cu_{Kα} radiation and a Ni filter, with a scan step of 0.0167° operated at 40 KV and 40 mA.

The kinetics and mechanism of formation of the Al-Si spinel phase were studied by two different methods isothermal and non-isothermal, each method give an excellent results. In the case of the non-isothermal method the activation energy (E_A) of crystallization is calculated using Ozawa-Flynn-Wall (OFW) (2) [8,9], Boswell (3) [10] and (4) for Kissinger-Akahira-Sunose (KAS) methods [2,5,11-14] as follows

$$\ln(\phi) = -1.0518 \frac{E_A}{RT_p} + C_1 \quad (2)$$

$$\ln\left(\frac{\phi}{T_p}\right) = -\frac{E_A}{RT_p} + C_2 \quad (3)$$

$$\ln\left(\frac{\phi}{T_p^2}\right) = -\frac{E_A}{RT_p} + C_3 \quad (4)$$

Where C_i ($i = 1, 2$ and 3) represents a constant, φ is the heating rate, E_A is the activation energy, T_p is the absolute peak temperature in DTA curves and R is the ideal gas constant. The value of kinetic exponent Avrami, n , can be calculated from the equation [5,13,15]:

$$n = \frac{2.5T_p^2 R}{w_{1/2} E_A} \quad (5)$$

Where $w_{1/2}$: is half-width (width at half high) of peak.

Matusita and coworkers have suggested a modified formula of the Kissinger equation [11,13] as

$$\ln\left(\frac{\phi^n}{T_p^2}\right) = C_3 - \frac{mE_A}{RT_p} \quad (6)$$

So n is the Avrami parameter indicates the crystallization mode and m is corresponding to a numerical factor depends on to the dimensionality of crystal growth.

The theoretical basis for the DTA results is provided under an isothermal condition using the Johnson-Mehl-Avrami (JMA) theory, this method describes

with the time, t , the evolution of the crystallisation fraction, x , during a phase transformation:

$$x = 1 - \exp\left[(-kt)^n\right] \quad (7)$$

x is the volume fraction crystallized after time (t), it was obtained from the DTA results presented in the formula as follow:

$$x = \frac{A_T}{A_0} \quad (8)$$

A_T is the area under the peak between the initial of crystallization T_i and the completion of crystallization T_f , A_0 is the total area of the peak in the DTA curve between the temperature T_i and T_f also k present the reaction rate constant.

Whose temperature dependence is mostly expressed by the Arrhenian-type equation [13]:

$$k = k_0 \exp\left(-\frac{E_A}{RT}\right) \quad (9)$$

So k_0 reveals the frequency factor, T in Kelvin is the isothermal temperature, E_A is the apparent activation energy and R is the ideal gas constant. The expression of formula (7) and (9) lead to:

$$\ln\left(\frac{dx}{dt}\right) = \ln[k_0 n] + \frac{n-1}{n} \ln[-\ln(1-x)] + \ln(1-x) - \frac{E_A}{RT} = \ln[k_0 f(x)] - \frac{E_A}{RT} \quad (10)$$

Through non-isothermal techniques Ligeró [11,13] proposed a mathematical method. The activation energy can be obtained from the slope of the equation (10) if we select the same value of x in every experiment on the applied heating rate, there must be a linear relationship between $\ln(dx/dt)$ and $1/T$ with slope gives the activation energy E_A . Then, it is possible to calculate the value of crystallized fraction x of the Al-Si spinel phase at various heating rates. Hence, the Avrami parameter n was calculated from the plot $\ln[k_0 f(x)]$ vs. $1/T$, we can choose many pairs of x_1 and x_2 that contented the condition $\ln[k_0 f(x_1)] = \ln[k_0 f(x_2)]$ and using equation (10), as the following equation [11,13]:

$$n = \frac{\ln\left[\frac{\ln(1-x_2)}{\ln(1-x_1)}\right]}{\ln\left[\frac{(1-x_2)\ln(1-x_2)}{(1-x_1)\ln(1-x_1)}\right]} \quad (11)$$

3 RESULTS AND DISCUSSION

The typical DTA/TG and DTA curves of Tamazarte kaolin powder is showing in Figure 1. The powder was heated from room temperature to 1400°C with

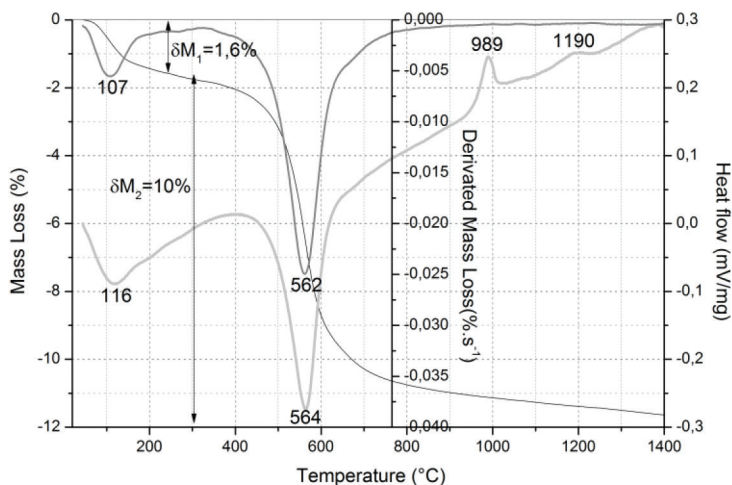


FIGURE 1
DTA/TG, DTG curves of Tamazarte kaolin powder heated at 20°C/min.

heating rate of 20°C/min. In the TG curve Two-step mass losses are observed clearly. The formation of kaolinite and the evaporation of adsorbed water is according to the first mass loss ($\Delta m = 1.6\%$). This process corresponds to the endothermic peak at 116°C as observed in the DTA curve and to first peak at 107°C as seen in the DTG curve. The second step equal to $\Delta m = 10\%$, this mass loss is due to the dehydroxylation of kaolinite and the formation of metakaolinite, that it's relates to the endothermic peak at 564°C seen in the DTA curve otherwise at 562°C, second peak, in the DTG curve. On the high temperature side on the DTA curve, two other exothermic peaks observed, the first one at 989°C, the metakaolinite is transformed to a spinel structure and amorphous silica SiO_2 . The AlO_6 group combine with SiO_4 groups in order to form the Al-Si spinel phase that, it was in a short range order structure. The Al-Si spinel phase appears at 930°C and continues until at least 1150°C. It is close to the value of temperature reported by H. Cheng et al. and Y. F. Chen et al. [3,16]. The last exothermic peaks at 1190°C due to the formation of mullite phase and the amorphous transformation of SiO_2 crystallizes to a crystalline phase (cristobalite) over 1200°C [1]. This new phase mullite increases with the heating temperature increasing from 1100 to 1200°C [3,17,18].

The thermodynamically stable mullite phase is forming by exothermic reaction over 1100°C and crystallization of cristobalite from amorphous silica proceeds subsequently. All the transformations of kaolin in DTA/DTG results are confirmed by the XRD phase analysis as shown in Figure 2.

Figure 2 reveals the XRD spectrum of raw kaolin (Tamazarte) as heated at various temperatures for 60 min. At ambient temperature, it is found that only reflections of kaolinite (K: aluminum silicate hydroxide $\text{Al}_2\text{Si}_2\text{O}_5(\text{OH})_4$) with constituents impurities such as quartz (Q: silicon oxide SiO_2) and mica

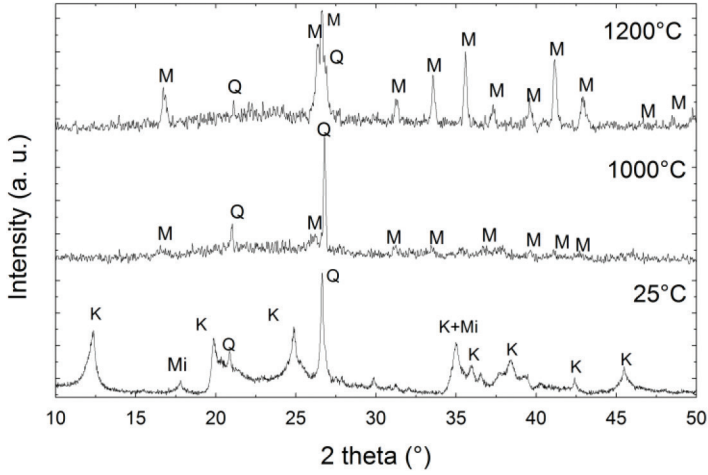


FIGURE 2

X-ray diffraction spectra of raw kaolin treated at different temperature (K: Kaolinite, Q: Quartz, Mi: mica muscovite, M: Mullite).

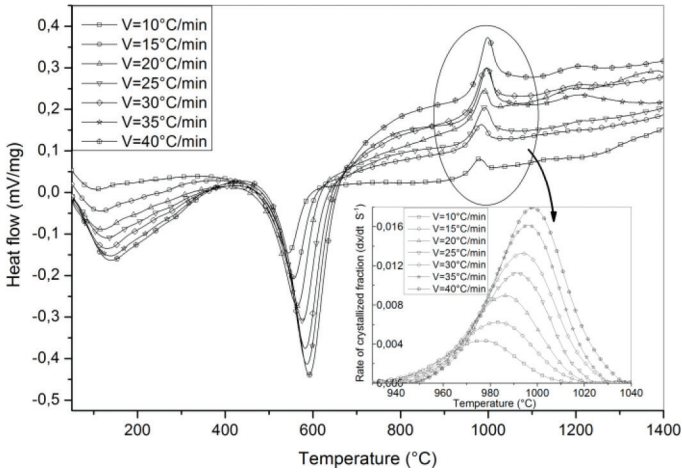


FIGURE 3

DTA curves of Tamazarte kaolin powder heated at different heating rates.

muscovite (Mi: $\text{KA}_2(\text{Si}_3\text{Al})\text{O}_{10} \cdot (\text{OH}, \text{F})_2$). At 1000°C mullite (M: $\text{Al}_6\text{Si}_2\text{O}_{13}$) phase starts to form from the Al–Si spinel phase which was formed and quartz impurities also detected. After this temperature the intensity of mullite increases with the heating temperature increasing until 1200°C.

Figure 3 depicts the DTA curves for Al–Si spinel phase at different heating rates and the rate of the crystallized fraction of Al–Si spinel phase under

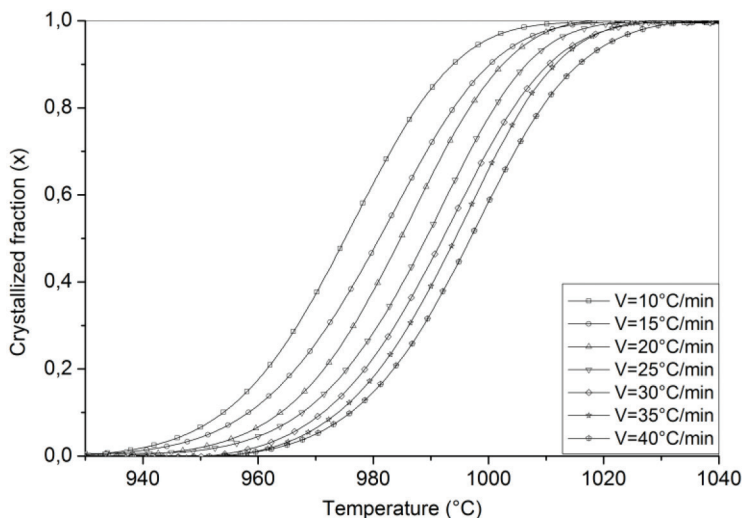


FIGURE 4
Crystallized fraction of Al-Si spinel formation under different heating rates.

applied heating rate using the differential thermal analysis (DTA). It can be observed that the temperature of the maximum of the exothermic peak, T_p , shifts to a higher temperature as the heating rate increases from 10 to 40°C otherwise the rate of the variation of the crystallized fraction increase from 0.004 to 0.018 s⁻¹.

Figure 4 represent the variation of the crystallized fraction of Al-Si spinel from Algerian Tamazarte kaolin studied by using differential thermal analysis (DTA) under different heating rates and by using equation (8). It can be seen that the time of the crystallized fraction decreases from 08 to 02 min when the heating rate increased from 10 to 40°C/min. The crystallized fraction x was determined from the DTA results as shown in Figure 3.

Figure 5 shows the plots of Y versus $1/T_p$ according to Ozawa (2), Boswell (3) and Kissinger (4) methods. The values of the activation energies of Al-Si spinel formation of Algerian Tamazarte kaolin at different heating rates by using DTA analyses calculated from the slope of the function $Y_i = f(1/T_p)$ were listed in Table 2. The average of activation energy is 806 kJ/mol. This value is in the range 550–954 kJ/mol of the activation energy determined [6,14,15,17,18] (they found 954, 822, 550, 840 and 856 kJ/mol, respectively). Additionally, it is considered that the presence of mica impurities in KT decrease the value of activation as reported by F. Sahnoune et al. [19] from 1260 kJ/mol to 806 kJ/mol.

Table 3 shows the values of the Avrami parameter which depicts the crystallization mode, n , for different heating rates was determined by using equation (5), the average Avrami parameter is 1.07 this value is close to 1 as

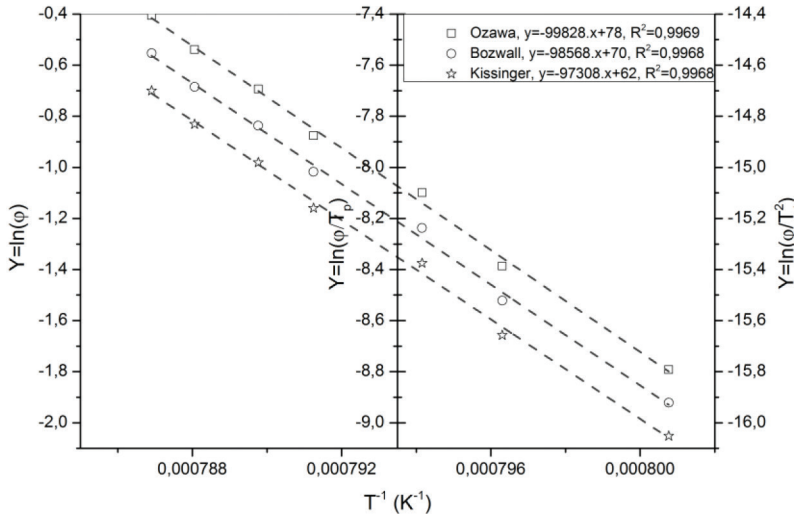


FIGURE 5
Plots of Y versus $(1/T_p)$ of Al-Si spinel formation at various heating rates.

TABLE 2

Values of E_A and R^2 of Al-Si spinel crystallized by using Ozawa, Boswell and Kissinger

Method	Ozawa	Boswell	Kissinger
The activation energy E_A (kJ/mol)	790	819	809
R^2	0.9969	0.9968	0.9968

TABLE 3

Values of the Avrami parameter n for different heating rates from DTA experiments

Heating rates	10°C/min	15°C/min	20°C/min	25°C/min	30°C/min	35°C/min	40°C/min
$w_{1/2}$	35.84	37.75	35.04	34.82	35.47	34.34	34.18
T_p peak	975.80	982.82	985.93	990.83	993.22	995.94	997.80
Avrami par.	1.04	1.02	1.08	1.09	1.08	1.12	1.07

reported in the table obtained by Matusita and Komatsu [20], which suggests, that the crystallization process of Al-Si spinel must be controlled by a diffusion growth.

Figure 6 represent the plots of $\ln(\varphi^n/T_p^2)$ versus $1/T_p$ according to Matusita (eq. 6). The dimensionality of crystal growth, m , calculated from the slope of the function, is found to be equal to 1.07 for the formation of Al-Si spinel phase. Both the growth morphology parameters n and m are equal to 1.07 which close to 1. These results showed that bulk nucleation was dominant in

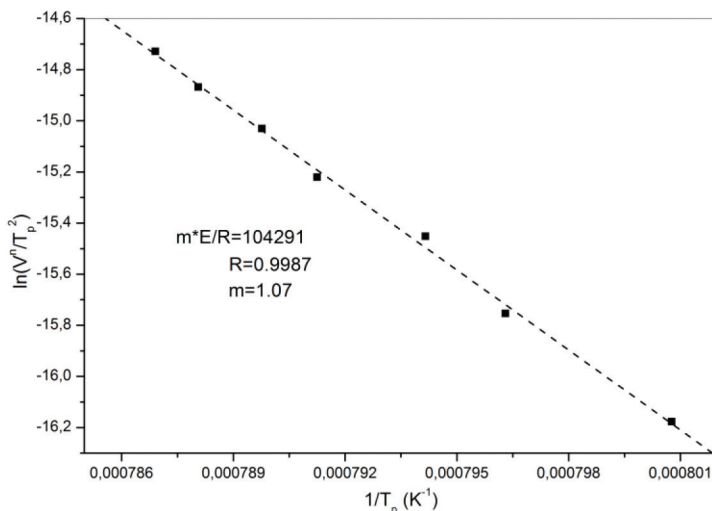


FIGURE 6
Plot of $\ln(\varphi^m/T_p^2)$ versus $1/T_p$ according to Matusita equation.

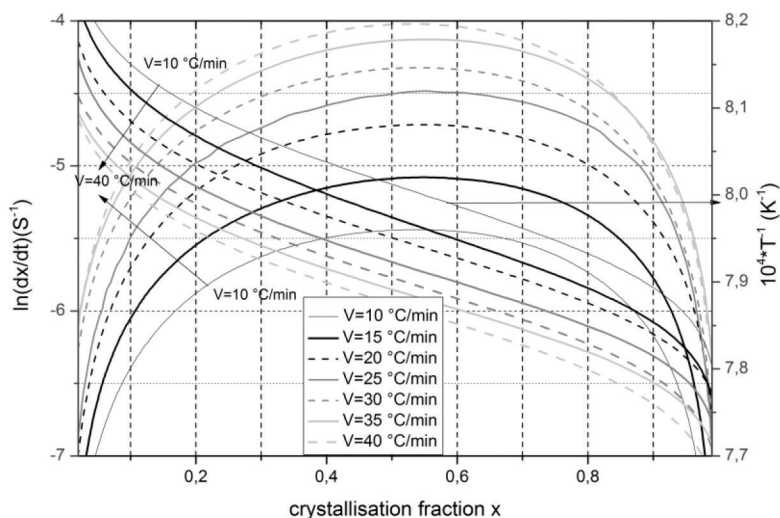


FIGURE 7
Plot of $Y = \ln(dx/dt)$ and $Y = 1/T$ versus of crystallized fraction x at different heating rates.

Al-Si spinel crystallization followed by Two-dimensional growth of mullite crystals with plates morphology controlled by diffusion from a constant number of nuclei [13,20].

Figure 7 presents the plot of $Y = \ln(dx/dt)$ and $Y = 1/T$ versus of crystallized fraction x at various heating rates from DTA experiment. At different

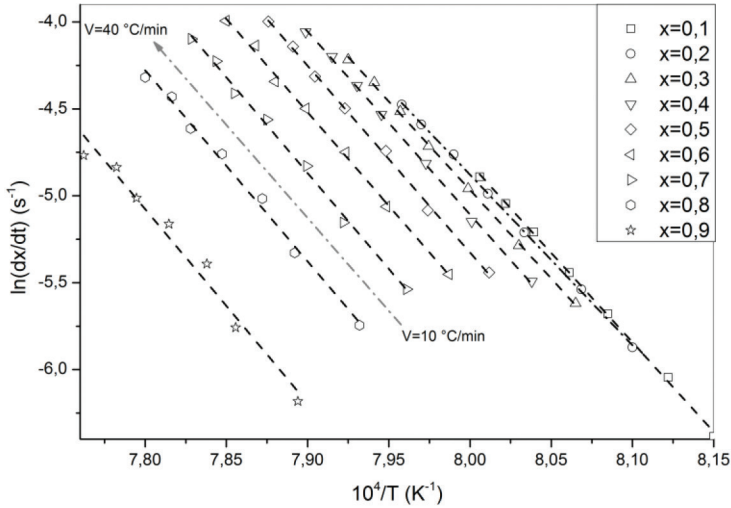


FIGURE 8
Plot of $\ln(dx/dt)$ versus $1/T$ at same value of crystallized fraction x at different rates.

TABLE 4
Values of E_A and R^2 for different crystallized fractions

Crystallized fractions x	0.1	0.2	0.3	0.4	0.5	0.6	0.7	0.8	0.9
R^2	0.998	0.999	0.999	0.998	0.998	0.996	0.995	0.992	0.970
E_A (kJ/mol)	848	869	837	852	869	870	890	888	900

heating rates (from 10 to 40°C/min) if the same value of crystallized fraction x in every experiment is selected and plot for each x given, the function $\ln(dx/dt)$ versus $1/T$ gives a linear curve Figure 8. The activation energy can be calculated from the slope of the function $\ln(dx/dt) = f(1/T)$. The values of activation energy E_A for a different crystallized fraction, which calculated by the average of the slopes of the lines, are registered in Table 4. The coefficient of determination R^2 is more than 0.99 for the different values of x . The average of activation energy Al–Si spinel formation is 875.6 kJ/mol, which is in agreement with the result obtained by non-isothermal DTA treatment that is 806 kJ/mol.

Figure 9 represents the plot of $\ln[k_0f(x)]$ versus crystallization fraction x for kaolin powder heated under applied heating rate (10, 20 and 30°C/min) which calculated for various heating rates with the knowledge of the activation energy. The Avrami parameter, n , was determined by the selection of various pairs of x_1 and x_2 that satisfy the condition $\ln[k_0f(x_1)] = \ln[k_0f(x_2)]$

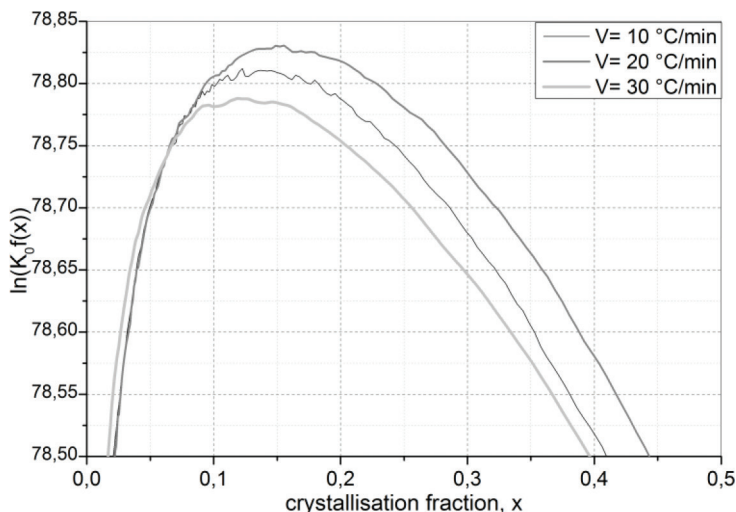


FIGURE 9
Plot of $\ln [k_0 f(x)]$ versus crystallization fraction for kaolin powder heated at different heating rates.

TABLE 5
Values of the Avrami parameter and $t_{0.75}/t_{0.25}$ value for different heating rates.

Heating rate (°C/min)	Avrami parameter, n	$t_{0.75}/t_{0.25}$ value
10	1.17	1.74
15	1.16	1.737
20	1.20	1.729
25	1.18	1.685
30	1.15	1.81
35	1.17	1.766
40	1.16	1.75

and using (eq. 11). The average values of Avrami parameter, n, for every heating rate were registered in Table 5. The average Avrami parameter is equivalent to $n = 1.17$.

The morphology of the crystal growth can be found, from the ratio of times for two fixed degrees of transformation [13,20]. A suitable representative index is the percentage of times for 75 and 25% transformation in such a way we find $2.20 \leq t_{0.75}/t_{0.25} \leq 4.82$ for one-dimensional growth (needles), $1.69 \leq t_{0.75}/t_{0.25} \leq 2.20$ for two-dimensional growth (plates) and $1.48 \leq t_{0.75}/t_{0.25} \leq 1.69$ for 3D growth (polyhedron). The middling values of $t_{0.75}/t_{0.25}$ for each heating rate are listed in Table 5. For all the heating rates the average value is equal to 1.75. This suggests a two-dimensional growth of Al-Si spinel crystallization [13,16].

4 CONCLUSIONS

The kinetics and mechanism of formation of the Al–Si spinel phase were studied using DTA technique. From the results the authors determined the following:

- The activation energies was calculated from the exothermic DTA peak from isothermal and non-isothermal treatments were around 875.6 and 806 kJ/mol, respectively.
- The Avrami parameters of growth morphology, n , were around 1 using non-isothermal and isothermal treatments.
- The numerical factor m , of crystal growth, is equal to be 1.07 and close to 1 using Matusita equation.

The bulk nucleation was followed by Two-dimensional growth of mullite crystals with plates morphology controlled by diffusion from a constant number of nuclei.

REFERENCES

- [1] De Aza A. H., Turrillas X., Rodriguez M. A., Duran T., Pena P. *J Eur Ceram Soc.* 34 (2014) 1409.
- [2] Traoré K., Gridi-Bennadji F., Blanchart P. *Thermochim Acta* 451 (2006) 99.
- [3] Cheng H. F., Liu Q. F., Yang J., Ma S., Frost R. L. *Thermochim Acta* 545 (2012) 1.
- [4] Chakraborty A. K. *Phase Transformation of Kaolinite Clay*. Springer India; 2014.
- [5] Ptáček P., Šoukal F., Opravil T., Havlica J., Brandštetr J. *Powder Technol.* 243 (2013) 40.
- [6] Ptáček P., Šoukal F., Opravil T., Nosková M., Havlica J., Brandštetr J. *J Solid State Chem.* 183 (2010) 2565.
- [7] Ptáček P., Šoukal F., Opravil T., Nosková M., Havlica J., Brandštetr J. *J Solid State Chem.* 184 (2011) 2661.
- [8] Ozawa T. *B Chem Soc Jpn.* 38 (1965) 1881.
- [9] Flynn J. H., Wall L. A. *J Res Nat Bur Stand.* 70A (1966) 487.
- [10] Boswell P. G. *J Therm Anal.* 18 (1980) 353.
- [11] Sahnoune F., Chegaar M., Saheb N., Goeuriot P., Valdivieso F. *Appl Clay Sci.* 38 (2008) 304.
- [12] Takei T., Kameshima Y., Yasumori A., Okada K. *J Eur Ceram Soc.* 21 (2001) 2487.
- [13] Romero M., Martín-Márquez J., Rincón J. Ma. *J Eur Ceram Soc.* 26 (2006) 164.
- [14] Sahnoune F., Saheb N., Khameh B., Takkouk Z. *J Therm Anal Calorim.* 107 (2012) 1067.
- [15] Ptáček P., Opravil T., Šoukal F., Havlica J., Holesinský R. *Solid State Sci.* 26 (2013) 53.
- [16] Chen Y-F., Wang M-C., Hon M-H. *J Eur Ceram Soc.* 24 (2004) 2389.
- [17] Prodanovic D., Živković Ž. D., Dumić M. *Thermochim Acta* 156 (1989) 61.
- [18] Kurajica S., Tkalcec E., Schmauch J. *J Eur Ceram Soc.* 27 (2007) 951.
- [19] Sahnoune F., Chegaar M., Saheb N., Goeuriot P., Valdivieso F. *Adv Appl Ceram.* 107 (2008) 9.
- [20] Matusita K., Miura K., Komatsu T. *Thermochim Acta* 88 (1985) 283.